

3-d Helimagnetic Metals are Analogous to 2-d Nonmagnetic Metals: Transport in the Ballistic Regime

T.R. Kirkpatrick¹, D. Belitz^{2,3}, and Ronojoy Saha²

¹*Institute for Physical Science and Technology and Department of Physics,
University of Maryland, College Park, MD 20742*

²*Department of Physics and Institute of Theoretical Science, University of Oregon, Eugene, OR 97403*

³*Kavli Institute for Theoretical Physics, University of California, Santa Barbara, CA 93106*

(Dated: April 21, 2019)

We present a quasi-particle model that allows for a simple many-body description of the electronic properties of metallic helimagnets. We apply this theory to the electrical conductivity for weak quenched disorder (ballistic regime), where we find the leading temperature dependence to be $T \ln T$ for bulk (3-d) materials. This is similar to the corresponding behavior of nonmagnetic 2-d systems, and it reflects a general feature that makes certain electronic properties of bulk metallic helimagnets appear effectively 2-d. This surprising prediction should be observable in weak helimagnets.

PACS numbers: 75.30.Ds; 75.30.-m; 75.50.-y; 75.25.+z

Helimagnets (e.g., MnSi and FeGe) form a class of magnetic materials where the magnetization displays ferromagnetic order in any plane perpendicular to a certain axis, but points in different directions depending on the position along that axis, forming a spiral. The metallic helimagnet MnSi in particular is a very well-studied material with many unusual properties. It shows helical order below a critical temperature $T_c \approx 30$ K with a helix wavelength $2\pi/q \approx 180$ Å [1]. Hydrostatic pressure decreases the helimagnetic transition temperature until the long-ranged helical order [2] disappears at a critical pressure $p_c \approx 14$ kbar [3]. At higher pressure, there is a phase or region where short-range helical order persists and the electrical resistivity shows a pronounced $T^{3/2}$ temperature dependence in a temperature range between a few mK and several K [4]. If this were the true asymptotic low-temperature behavior, it would represent non-Fermi liquid behavior in a bulk material with no long-range order, which would be very remarkable.

The $T^{3/2}$ behavior is not observed in the ordered phase. Nevertheless, fluctuations of the helix that couple to the electrical conductivity are an obvious possible source for unusual transport behavior, and it is natural to first study the effects of helimagnon excitations in the ordered phase to understand their potential effects more generally [5]. It was recently shown that massless excitations of the helix, helimagnons, do indeed lead to a non-analytic temperature dependence of the resistivity in the ordered phase [6]. However, for the most interesting observables in a clean system these effects provide *corrections* to the usual Fermi-liquid behavior: the leading helimagnon contribution to the resistivity has a $T^{5/2}$ behavior, and the specific heat goes as T^2 , although the single-particle relaxation rate goes as $T^{3/2}$. In this paper we make a prediction for the resistivity in bulk (3-d) samples with a small concentration of nonmagnetic impurities. We show that in a certain regime the leading temperature dependence of the resistivity is $T \ln T$. Remarkably, this

is much stronger than either the $T^{5/2}$ clean helimagnon contribution or the T^2 Fermi-liquid contribution, and it is reminiscent of the behavior of two-dimensional (2-d) nonmagnetic metals.

The samples used in Ref. 4 have a residual resistivity of about $0.3 \mu\Omega\text{cm}$. At the experimentally attainable temperatures, this places them in the ballistic regime, $T\tau \gg 1$, with τ the elastic mean-free time, where the transport is governed by free-electron motion in between rare scattering events, as opposed to diffusive motion in the opposite limit, $T\tau \ll 1$. The ballistic regime has been investigated by Zala et al. [7] for the case of electrons interacting via a screened Coulomb interaction in 2-d metals, where they found a linear dependence of the resistivity on the temperature. (In 3-d, the corresponding resistivity correction is of $O(T^2)$.) Although the ballistic regime is never the true asymptotic low-temperature regime, it thus can display very unusual behavior. Furthermore, depending on the impurity concentration in the sample, it can represent the low- T asymptotics for practical purposes. In this Letter we investigate the transport behavior in bulk metallic helimagnets due to the scattering of electrons by helimagnons. Our main result is that 3-d helimagnets behave rather similarly to 2-d nonmagnetic metals, with the leading temperature dependence of the resistivity in the ballistic regime (which is defined slightly differently than in the Coulomb case, see below) given by $T \ln T$.

Transport theory for helimagnets is rather complicated even in the clean case if the Kubo formula is evaluated using the usual plane-wave basis. In this basis, the electronic Green function is not diagonal in either wave vector space or spin space, which makes for very cumbersome calculations [6]. Including impurity scattering in this formalism would be hard. However, several features of this theory, which we quote below, suggest a much simpler effective description. The poles of the electronic Green

function, or quasi-particle (QP) energies, are given by

$$\omega_{1,2}(\mathbf{k}) = \frac{1}{2} \left(\xi_{\mathbf{k}} + \xi_{\mathbf{k}+\mathbf{q}} \pm \sqrt{(\xi_{\mathbf{k}} - \xi_{\mathbf{k}+\mathbf{q}})^2 + 4\lambda^2} \right). \quad (1)$$

Here $\xi_{\mathbf{k}} = \epsilon_{\mathbf{k}} - \epsilon_F$, with $\epsilon_{\mathbf{k}}$ the electronic energy-momentum relation and ϵ_F the chemical potential. For a cubic crystal, such as MnSi,

$$\epsilon_{\mathbf{k}} = \frac{\mathbf{k}^2}{2m_e} + \frac{\nu}{2m_e k_F^2} (k_x^2 k_y^2 + k_y^2 k_z^2 + k_z^2 k_x^2) + O(k^6), \quad (2)$$

with m_e the effective electron mass, and $\nu = O(1)$ a dimensionless measure of deviations from nearly free electrons. We choose units such that $\hbar = k_B = e = 1$.

$\mathbf{q} = (0, 0, q)$ is the helix pitch vector, which we choose to point in the z -direction, and λ is the Stoner splitting. The two signs of the square root represent the two Stoner bands, and for $\mathbf{q} = 0$ one recovers the usual ferromagnetic result in Stoner approximation. Excitations between the two Stoner bands will be gapped by λ , and we can thus restrict ourselves to a single band by considering spinless QPs with resonance frequency $\omega_1(\mathbf{k})$.

For the electronic QP Green function one thus expects

$$G_0(p) = 1/(i\omega_n - \omega_1(\mathbf{p})), \quad (3)$$

where $p = (\mathbf{p}, i\omega_n)$ with ω_n a fermionic Matsubara frequency [8]. We have shown that such a QP Green function can indeed be derived from a canonical transformation to suitable fermionic degrees of freedom $\eta(p)$ [9]. The soft, or massless, helical degrees of freedom, the helimagnons, are fluctuations of a generalized helical phase ϕ with a frequency

$$\omega_0(\mathbf{p}) = \sqrt{c_z p_z^2 + c_{\perp} p_{\perp}^4}. \quad (4a)$$

Here p_z and p_{\perp} are the longitudinal and transverse components, respectively, of the wave vector with respect to the pitch wave vector \mathbf{q} , and the elastic constants c_z and c_{\perp} are given by

$$c_z \propto \lambda^2 q^2/k_F^4, \quad c_{\perp} \propto \lambda^2/k_F^4. \quad (4b)$$

Equation (4a) is valid for $|\mathbf{p}| < q$. Notice that the helimagnon dispersion relation is anisotropic: it is ferromagnet-like in the longitudinal direction, but antiferromagnet-like in the transverse direction. The helimagnon susceptibility is given by

$$\chi(k) = \langle \phi(k) \phi(-k) \rangle = \frac{1}{2N_F} \frac{q^2/3k_F^2}{\omega_0^2(\mathbf{k}) - (i\Omega_n)^2}, \quad (5)$$

with Ω_n a bosonic Matsubara frequency, $k = (\mathbf{k}, i\Omega_n)$, and N_F the density of states at the Fermi level. We see that frequency or temperature scale with the soft wave vector \mathbf{k} as $T \sim k_z \sim k_{\perp}^2$.

Since ϕ is a phase, only the gradient of ϕ is of physical significance and will couple to the QPs. Furthermore, the

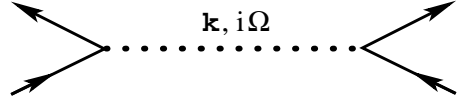


FIG. 1: Effective interaction between QPs (solid lines) by exchange of a helimagnon (dotted line). Notice that the interaction depends on the momenta of the QPs.

results of Ref. 6 show that the leading coupling is not to the QP density, but rather to the $z \perp$ components of the QP stress. Upon integrating out ϕ , one thus expects an effective potential for the interaction of QPs by means of exchange of helimagnons that is given pictorially in Fig. 1, and analytically by

$$V_{\text{eff}} = -\lambda^2 (q^2/m_e^2) \chi(k) \gamma(\mathbf{k}, \mathbf{p}) \gamma(\mathbf{k}, \mathbf{p}'), \quad (6a)$$

where

$$\gamma(\mathbf{k}, \mathbf{p}) = \nu p_z (\mathbf{p}_{\perp} \cdot \mathbf{k}_{\perp}) \quad (6b)$$

is a vertex function.

Finally, we expect static impurities or quenched disorder to couple to the QP density. Putting everything together, we now have the following effective action:

$$S = S_0 + S_{\text{int}} + S_{\text{dis}}, \quad (7a)$$

where

$$S_0 = (T/V) \sum_p \bar{\eta}(p) [i\omega_n - \omega_1(p)] \eta(p) \quad (7b)$$

describes free QPs,

$$\begin{aligned} S_{\text{int}} = & \frac{T}{V} \sum_k \frac{1}{V^2} \sum_{\mathbf{p}, \mathbf{p}'} V_{\text{eff}}(k; \mathbf{p}, \mathbf{p}') T \sum_{i\omega} \bar{\eta}(\mathbf{p}, i\omega) \\ & \times \eta(\mathbf{p} + \mathbf{k}, i\omega + i\Omega) \bar{\eta}(\mathbf{p}', i\omega) \eta(\mathbf{p}' - \mathbf{k}, i\omega - i\Omega) \end{aligned} \quad (7c)$$

describes the effective QP interaction via the exchange of a helimagnon, and

$$S_{\text{dis}} = (-1/V^2) \sum_{\mathbf{k}, \mathbf{p}} u(\mathbf{k} - \mathbf{p}) T \sum_{i\omega} \bar{\eta}(\mathbf{k}, i\omega) \eta(\mathbf{p}, i\omega) \quad (7d)$$

describes the quenched disorder. Here u is a delta-correlated point-like random potential with a Gaussian distribution whose second moment is given by $1/2\pi N_F \tau$.

The Eqs. (7) represent an effective model for QPs interacting via a dynamical potential that allows for many-body perturbation theory, and an evaluation of the Kubo formula in particular, in complete analogy to electrons interacting via a dynamically screened Coulomb interaction. The only unusual aspects are, (1) the coupling to the QP stress rather than the density, and (2) the anisotropic nature of the exchanged excitations. The former is embodied in the vertex functions γ in Eqs. (6)

and easy to handle technically. The latter makes the bulk system behave in some respects like a 2-d system, as we will see below. This effective model is much simpler to handle than the model studied in Ref. 6. We have derived the former from the latter by means of a canonical transformation [9]; the above considerations represent just plausibility arguments for the effective model.

Transport theory now proceeds in analogy to the Coulomb problem. In order to calculate the static electrical conductivity tensor σ_{ij} we evaluate the Kubo formula

$$\sigma_{ij} = -\lim_{\Omega \rightarrow 0} \text{Re} \frac{i}{i\Omega_n} \int_0^{1/T} d\tau e^{i\Omega_n \tau} \left\langle T_\tau \hat{j}_i(\mathbf{k}, \tau) \times \hat{j}_j(\mathbf{k}, \tau = 0) \right\rangle \Big|_{i\Omega_n \rightarrow \Omega + i0, \mathbf{k} = 0}, \quad (8)$$

with $\hat{j}(\mathbf{k}, \tau)$ the current operator in imaginary-time representation and T_τ the imaginary time ordering operator. The tensor σ_{ij} is diagonal and has two independent elements, $\sigma_L \equiv \sigma_{zz}$ and $\sigma_\perp \equiv \sigma_{xx} = \sigma_{yy}$.

In the clean limit, $\tau \rightarrow \infty$, the analysis reproduces the results of Ref. 6. Specifically, an infinite ladder resummation of both the self-energy and vertex-correction contributions to the conductivity shows that the leading low- T terms cancel between the two sets of diagrams. As a result, the transport relaxation rate, and hence the resistivity, shows a $T^{5/2}$ behavior, whereas the single-particle relaxation rate goes as $T^{3/2}$.

In the ballistic limit, it is convenient to include the disorder in the Green function in the Born approximation, i.e., to use a Green function

$$G(p) = 1/(i\omega_n - \omega_1(\mathbf{p}) + i \text{sgn}(\omega_n)/2\tau) \quad (9)$$

instead of Eq. (3). The diagrams that contribute to the correction to the conductivity to leading order in the disorder in the ballistic limit are shown in Fig. 2; they are the same as in Ref. 7.

Diagrams (i) and (ii) also contribute in the clean limit, where there respective ladder resummations must be taken into account. In the presence of disorder, their leading terms are proportional to $\tau^2 T^{3/2}$. (This is just the result of adding the clean single-particle rate, which is proportional to $T^{3/2}$, to $1/\tau$ according to Matthiessen's rule, and expanding.) These terms cancel between the self-energy diagram (i) and the vertex-correction diagram (ii), as they must according to Ref. 6. An inspection of the integrals shows that the small parameter for the disorder expansion is $\epsilon = 1/\sqrt{\tau^2 T \epsilon_F^2 / \lambda}$. This is different from the Coulomb case, where the small parameter is $1/\tau T$ [7]. Consequently, the next-leading terms are of order τT . These also cancel between the two diagrams.

The remaining diagrams all carry an explicit factor of $1/\tau$, so it suffices to calculate their leading behavior, and they can be classified with respect to their momentum structure. They each contain six Green functions that factorize into two correlation functions formed by n and

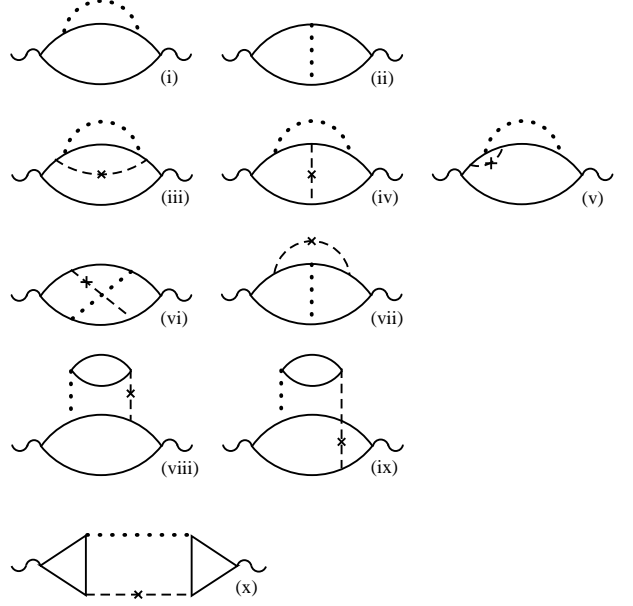


FIG. 2: Leading contributions to the conductivity in the ballistic limit. Solid lines represent the Green function given by Eq. (9), dotted lines represent the effective potential, Eqs. (6), and dashed lines represent the impurity factor $1/2\pi N_F \tau$. Obvious symmetric counterparts of all diagrams except (ii) are not shown. See the text for additional information.

$6 - n$ Green functions, respectively, with $n = 3$ or $n = 4$. Power counting shows that the (4, 2) partitions are smaller than the (3, 3) partitions by a factor of $(q/k_F)^2$. Dropping the former leaves us with diagrams (iii), (iv), (vi), and (x). Furthermore, power counting reveals that for σ_\perp , only diagram (iii) is of $O(\tau T)$. An inspection of the integral shows a logarithmic singularity that is cut off by ϵ . For σ_L , diagrams (iv) and (vi) also contribute to $O(\tau T)$, but the terms that contain a $\ln \epsilon$ cancel between the two diagrams. Finally, the leading contribution to diagram (x) vanishes due to reality requirements.

We thus conclude that the leading contributions to both the longitudinal and the transverse conductivity corrections are given by diagram (iii) alone. We find

$$\delta\sigma_L = \delta\sigma_\perp = -\sigma_0 \frac{4\sqrt{6}\pi^2}{3} \nu^2 \left(\frac{\epsilon_F}{\lambda}\right)^2 \left(\frac{q}{k_F}\right)^3 \times [1 + O((q/k_F)^2)] \frac{T}{\epsilon_F} [\ln(\tau^2 T \epsilon_F^2 / \lambda) + O(1)], \quad (10)$$

with $\sigma_0 = (2k_F/3\pi^2) \epsilon_F \tau$ the Drude conductivity. Notice that for the ballistic correction there is no cancellation between self-energy and vertex correction contributions; the corrections to both the single-particle rate and the transport rate are proportional to $T \ln T$.

We now discuss this result. The ballistic temperature regime is bounded below by the requirement that the expansion parameter ϵ be small, i.e., $T\tau^2 \epsilon_F^2 / \lambda \gg$

1. This defines a temperature scale $T_{\text{ball}} = \lambda/(\epsilon_F\tau)^2$. It is bounded above by the ballistic correction to the relaxation rate crossing over to either the clean-limit rate $1/\tau_{\text{clean}} \propto T^{5/2}$ [6], or to the Fermi-liquid rate $\tau_{\text{FL}} \approx T^2/\epsilon_F$. For the former, we have a crossover temperature $T_{1-5/2} = \lambda/(\epsilon_F\tau)^{2/3}$, for the latter, $T_{1-2} = (1/\tau)(q/k_F)^3(\epsilon_F/\lambda)^2$. The ballistic rate thus yields the dominant T dependence of the resistivity in the regime

$$T_{\text{ball}} \ll T \ll \text{Min}(T_{1-2}, T_{1-5/2}), \quad (11)$$

and $T_{1-2}/T_{1-5/2} = (q/k_F)^3(\epsilon_F/\lambda)^3/(\epsilon_F\tau)^{1/3}$. If $\lambda \lesssim \epsilon_F$, then $T_{1-2} \ll T_{1-5/2}$. In a weak helimagnet, where λ/ϵ_F might be as small as q/k_F , we still have $T_{1-2} < T_{1-5/2}$ on account of the factor $1/(\epsilon_F\tau)^{1/3}$. For realistic parameter values, the ballistic regime will thus be

$$T_{\text{ball}} \ll T \ll T_{1-2} = T_{\text{ball}}(\epsilon_F\tau)(q/k_F)^3(\epsilon_F/\lambda)^3. \quad (12)$$

The upper limit depends strongly on ϵ_F/λ , which is often not well known. For weak helimagnets, with $\lambda \ll \epsilon_F$, it is possible to have $T_{1-2} \gg T_{\text{ball}}$ by virtue of $\epsilon_F\tau \gg 1$. For larger values of λ the ballistic correction may never dominate unless the system is extremely clean. In that case, one will have to subtract the Fermi-liquid T^2 behavior in order to observe the ballistic contribution. For MnSi, with $\epsilon_F \approx 23,000$ K and $\epsilon_F\tau \approx 1,000$ for the samples of Ref. 4, one has $T_{\text{ball}} \approx 10$ mK. $q/k_F \approx 0.02$, but the value of λ is not well known. For the upper and lower limits used in Ref. 6, namely, $\lambda = \epsilon_F/2$ and $\lambda = 540$ K, respectively, we find $T_{1-2} \approx 0.06 T_{\text{ball}}$ and $T_{1-2} \approx 500 T_{\text{ball}}$, which again underscores the strong dependence on ϵ_F/λ . Generally speaking, weak helimagnets are the best candidates for observing the ballistic transport regime.

The reason for our result for a 3-*d* system being qualitatively similar to that for a 2-*d* one with just a Coulomb interaction [7] can be traced back to the anisotropic helimagnon dispersion relation, Eq. (4a). The basic point is that the components of the soft wave vector \mathbf{k} scale as $k_z \sim k_{\perp}^2 \sim T$. The relevant integrals that determine observables are of the form

$$\int dk_z \int d\mathbf{k}_{\perp} \mathbf{k}_{\perp}^2 \delta(\Omega^2 - k_z^2 - \mathbf{k}_{\perp}^2) f(k_z, \mathbf{k}_{\perp}) \propto \int d\mathbf{k}_{\perp} \mathbf{k}_{\perp}^2 \frac{\Theta(\Omega^2 - \mathbf{k}_{\perp}^4)}{\sqrt{\Omega^2 - \mathbf{k}_{\perp}^4}} f(k_z = 0, \mathbf{k}_{\perp}),$$

where f is a scalar-valued function of \mathbf{k} , and its dependence on k_z can be dropped since it does not contribute to the leading temperature scaling. The prefactor of the \mathbf{k} dependence of f is of $O(1)$ in a scaling sense. As a result, the 3-*d* integral over \mathbf{k} behaves effectively like the integral in the 2-*d* Coulomb case [10].

Finally, we point out a generic feature relevant for the explanation of the $T^{3/2}$ behavior observed in the disordered phase of MnSi. The prefactor of T/ϵ_F in $\delta\sigma/\sigma_0$,

Eq. (10), is very small. Assuming $\nu = 1$ and the above parameter values for MnSi, it is about 10^{-3} for $\lambda = \epsilon_F/2$, and about 0.54 for $\lambda = 540$ K, ignoring the log. The latter provides a factor of up to 10 in the temperature regime $T \approx 1$ K. The small prefactor reflects the long wavelength of the helix on a microscopic scale. The prefactor of the $T^{5/2}$ behavior in the clean limit is also small, for the same reason. By contrast, the prefactor of the experimentally observed $(T/\epsilon_F)^{3/2}$ behavior of the resistivity in the disordered phase is of $O(10^6)$. We conclude that whatever is causing the $T^{3/2}$ behavior of the transport rate in MnSi must be due to processes on short length scales, and is unlikely to be related to the helical order.

In conclusion, in the ordered phase of metallic helimagnets we predict that at low temperatures in the ballistic regime, the leading temperature correction to the Drude conductivity is proportional to $T \ln T$. This result should be most easily observable in weak helimagnets.

This research was supported by the National Science Foundation under Grant Nos. DMR-05-30314, DMR-05-29966, and PHY05-51164.

- [1] Y. Ishikawa, K. Tajima, D. Bloch, and M. Roth, Solid State Commun. **19**, 525 (1976).
- [2] Strictly speaking, there never is any true long-range helical order at any nonzero temperature due to strong fluctuations of the helix, see Ref. 11. However, this is a weak effect that we will neglect for our present purposes.
- [3] C. Pfleiderer, G. J. McMullan, S. R. Julian, and G. G. Lonzarich, Phys. Rev. B **55**, 8330 (1997).
- [4] C. Pfleiderer, S. R. Julian, and G. G. Lonzarich, Nature **414**, 427 (2001).
- [5] In a rotationally invariant model, effects of helical fluctuations will be strongest in the ordered phase. In a crystal, crystal-field effects will pin the helix, which makes the helical excitations massive. Such pinning is expected to disappear in a phase where the helical order is destroyed, but still persists on some length scales. A rotationally invariant model of the ordered phase may therefore provide a reasonable description of the high-pressure phase.
- [6] D. Belitz, T. R. Kirkpatrick, and A. Rosch, Phys. Rev. B **74**, 024409 (2006).
- [7] G. Zala, B. N. Narozhny, and I. L. Aleiner, Phys. Rev. B **64**, 214204 (2001).
- [8] It is not obvious that it is possible to find a quasi-particle description where the Green function is diagonal in momentum space. However, the canonical transformation mentioned in the text shows that it is.
- [9] T. R. Kirkpatrick, D. Belitz, and Ronjoy Saha, unpublished results.
- [10] It is important for this argument that there is no qualitative difference between a stress coupling and a density coupling. This is true in the ballistic limit but not, for instance, in the diffusive limit.
- [11] T. R. Kirkpatrick and D. Belitz, Phys. Rev. Lett. **97**, 267205 (2006).